

ACKNOWLEDGMENT

The authors wish to thank Dr. S. Algeri, Dr. M. G. De Simoni of Istituto di Ricerche Farmacologiche Mario Negri, Milan, Italy, and Dr. L. Imeri of Istituto di Fisiologia Umana II, University of Milan, Milan, Italy, for the experiments on live animals and the discussion of results.

REFERENCES

- [1] M. M. Zeeman and C. L. Perrin, *Organic Polarography*. New York: Interscience, 1969.
- [2] See, e.g., M. G. De Simoni, G. Dal Toso, F. Fodritto, A. Sokola, and S. Algeri, "Modulation of striatal dopamine metabolism by the activity of dorsal Raphe serotonergic afferences," *Brain Res.*, vol. 411, pp. 81-88, Feb. 1987.
- [3] See, e.g., Ikada, H. Miyazaky, and A. Matsushita, "Simultaneous monitoring of electrochemical and unitary neuronal activities by a single carbon fiber microelectrode," *Japan. J. Pharm.*, vol. 37, pp. 303-305, Apr. 1985.
- [4] A. G. Ewing, K. D. Alloway, S. D. Curtis, M. A. Dayton, R. M. Wightman, and G. V. Rebec, "Simultaneous electrochemical and unit recording measurements: Characterization of the effects of D-amphetamine and ascorbic acid on neurostriatal neurons," *Brain Res.*, vol. 261, pp. 101-108, Feb. 1983.
- [5] V. Annovazzi-Lodi and S. Donati, "An optoelectronic interconnection for bidirectional transmission of biological signals," *IEEE Trans. Biomed. Eng.*, vol. 35-8, pp. 595-606, Aug. 1988.
- [6] M. G. De Simoni, A. De Luigi, L. Imeri, and S. Algeri, "Miniaturized optoelectronic system for telemetry of *in vivo* voltammetric signals," *J. Neurosc. Meth.*, to be published.

Design and Calibration of a High-Frequency Oscillatory Ventilator

Brett A. Simon and Wayne Mitzner

Abstract—High-frequency ventilation (HFV) is a modality of mechanical ventilation which presents difficult technical demands to the clinical or laboratory investigator. The essential features of an ideal HFV system are described, including wide frequency range, control of tidal volume and mean airway pressure, minimal dead space, and high effective internal impedance. The design and performance of a high-frequency oscillatory ventilation system is described which approaches these requirements. The ventilator utilizes a linear motor regulated by a closed loop controller and driving a novel frictionless double-diaphragm piston pump. Finally, the ventilator performance is tested using the impedance model of Venegas [1].

INTRODUCTION

High-frequency ventilation (HFV) is a relatively new form of mechanical ventilation which operates at supranormal (1-30 Hz) frequencies (f) while using tidal volumes (V_T) equal to or smaller than the anatomic dead space. The ability of these systems to adequately oxygenate and ventilate both humans and experimental animals is well documented [2]-[4]. A large variety of HFV systems have been used [1], [5]-[7], and, while each has its advantages and disadvantages, it is clear that an ideal system should have

Manuscript received September 19, 1988; revised December 26, 1989.

The authors are with the Departments of Biomedical Engineering and Environmental Health Sciences, The Johns Hopkins Medical Institutions, Baltimore, MD 21205.

IEEE Log Number 9041293.

certain characteristics. These features include wide frequency range, easily controlled and reproducible tidal volume, minimum equipment dead space, independently controlled mean airway pressure or lung volume, and variable inspiratory: expiratory time ratio. The ventilator should also have an effective high "internal impedance," as described by Venegas [1], so that its output is relatively insensitive to changes in respiratory system impedance.

In this communication we describe a high-frequency oscillatory ventilator which approaches the above requirements. It uses a linear motor regulated by a second-order closed-loop controller and driving a novel frictionless double-diaphragm piston-cylinder pump. Mean airway pressure is controlled by a servo-control valve on the bias flow outlet, and tidal volume is measured by an in-line pneumotachograph. The design and implementation of this system are described emphasizing the application of general engineering techniques and principles, and the ventilator performance is tested using the impedance model of Venegas [1].

GENERAL DESCRIPTION

The high frequency ventilation system used is schematically pictured in Fig. 1. It is a bias-flow oscillator system, with regulation of mean airway pressure (P_{aw}) by a servo-control valve on the vacuum line. The ventilator itself consists of a linear "voice coil" motor (Infomag model 15) driven by a second-order closed-loop controller (see below). The motor drives a lightweight hollow aluminum piston which is sealed to the Plexiglas cylinder with back to back rolling diaphragms (Bellofram Corp., Burlington, MA); there are no friction seals. With a piston cross-sectional area of 45 cm² this system is able to deliver tidal volumes over 50 mL at 25 Hz and up to 100 mL at frequencies below 5 Hz. Other advantages of this design include the elimination of piston dead space at all tidal volumes, continuously variable frequency and tidal volumes, minimization of piston-cylinder alignment problems, and the ability to follow arbitrary input waveforms.

HFV was delivered through a 23-cm-long 2.5-cm-diameter straight Plexiglas tube which was connected to the endotracheal tube via a tapered rubber connector. P_{aw} was measured via a small flush sidearm at the center of this conduit with a Validyne DP45 transducer (± 140 cm H₂O). This arrangement has been shown to minimize the errors associated with airway pressure measurement during HFV [8]. The fresh air bias flow entered through a small opening at the dog end and exited through another at the piston end of the plexiglas tube. A bias flow rate of 8 L/min, measured with a Matheson Mass Flowmeter (Model 8160, Matheson Co., E. Rutherford, NJ), was used in all experiments. The pressure transducer signal was amplified and filtered with a Validyne CD100-3 carrier amplifier and used as the input to a Brown Electrodynamic servo amplifier, which controlled a valve between the bias flow exhaust and a vacuum source to regulate P_{aw} . This simple linear feedback P_{aw} controller was empirically adjusted to be slightly underdamped, so that P_{aw} was restored smoothly within 3-4 s after a step change in the input or a transient disturbance.

MECHANICAL SPECIFICATIONS

A. Linear Motor

This type of motor consists of a permanent toroidal magnet and a cylindrical coil which moves freely along its axis. Current running through the coil causes it to exert a proportional force along the axis of the magnet. An Infomag model 15 linear motor was used which has a force constant of 2.9 lb/amp, a constant force stroke of 5 cm (total stroke 9.1 cm), and a maximum power dissipation (air cooled) of 280 W. The coil was mounted on a 3/8 in aluminum shaft and was supported on two linear ball bearing bushings which were press fit into the 5/8 in axial bore of the motor housing: no

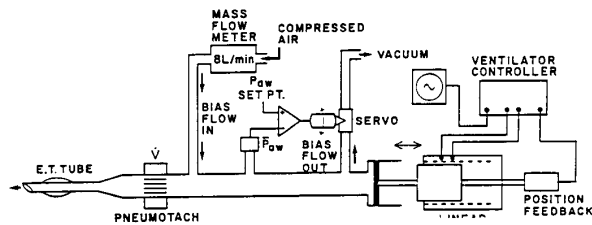


Fig. 1. Schematic representation of high-frequency ventilation system, including linear motor ventilator, bias flow with servo control of mean airway pressure, and pneumotachograph for tidal volume measurement. See text for details.

additional external supports were needed. This arrangement had very low friction and minimized the moving mass.

B. Double Diaphragm Piston

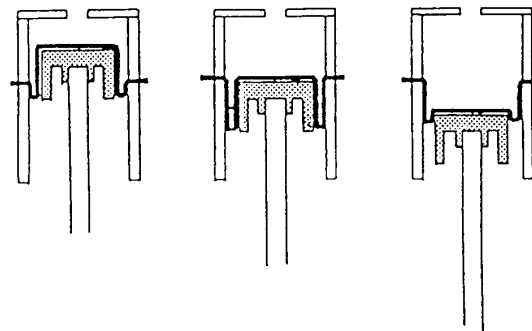
The objective of piston design is to minimize friction while maintaining a perfect seal and avoiding the problem of piston-cylinder misalignment. Standard designs using O-rings require smooth and round cylinder walls, periodic lubrication, yet still have considerable friction and are sensitive to misalignment. The use of "rolling diaphragm" seals provides a solution to these problems. The diaphragms are made of a high tensile strength woven fabric impregnated with an elastomer. The principle of operation is diagrammed in Fig. 2(a). Note that there is clearance between the piston and cylinder walls. The diaphragm looks like a "top hat" with a rim, sides, and flat top. The rim is clamped within the cylinder walls, the top clamped to the piston face, and the sides loop down or "convolute" between the piston and cylinder walls. As the piston moves back and forth the sides of the diaphragm roll with it; the seal is maintained by the continuous diaphragm surface with minimal friction, resulting only from the continuous deformation of the diaphragm margins. However, during the piston backstroke the chamber pressure could become negative and evert the diaphragm convolution. To prevent this event, a second diaphragm was added back-to-back to the first and the sealed chamber between them connected to a negative pressure source, usually wall vacuum [9]. This modification maintains both diaphragms in continuous tension without causing additional loading of the motor.

The mechanical design of the piston and cylinder is shown in Fig. 2(b). Bellofram model 4-300-119-DBJ diaphragms (generously provided by the Bellofram Corporation, Burlington, MA), had an effective piston area of 45 cm² with a maximum 5 cm stroke. The cylinder was constructed of stock 3 1/2 in diam Plexiglas tubing which was bored out to 3 in i.d. The piston was machined from aluminum and features a thin walled 2 in long skirt and end caps which clamp the top of the two diaphragms securely to the piston faces [10]. Precise alignment was not important because of the clearance between the piston and cylinder, a factor which makes changing the diaphragms in case of failure relatively easy.

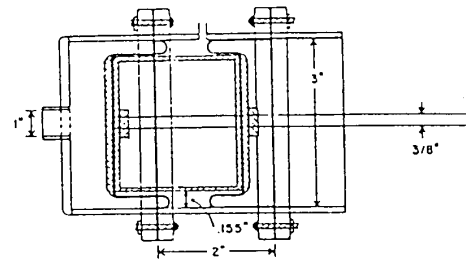
CONTROL SYSTEM SPECIFICATIONS

It was anticipated that both position and velocity feedback would be required to get the desired performance from this system, so a simple second-order feedback controller with variable gains was designed (Fig. 3). Position feedback was obtained from a linear film-type potentiometer (Waters Manufacturing Co., Wayland, MA) connected to the ventilator shaft. The velocity signal was obtained by differentiation of this position signal with a simple RC op amp circuit which acted as a pure differentiator over the frequency range 1-100 Hz. Its performance, expressed as a transfer function, was characterized by

$$G_D = -s/312 \quad (1)$$



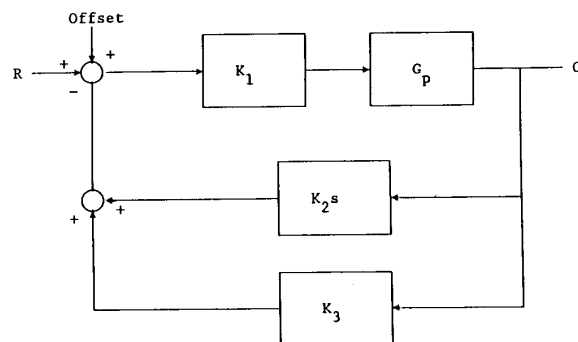
(a)



(b)

Fig. 2. (a) Principle of operation of "rolling diaphragm" seals used in HFV ventilator. There is clearance between the piston skirt and cylinder walls; the continuous diaphragm rolls in that space as the piston moves, maintaining a seal with a minimum of friction. (b) Detailed mechanical drawing of piston/cylinder arrangement. Two back-to-back diaphragms, with the closed space in between connected to wall vacuum, were used to prevent the forward seal from everting due to negative chamber pressure created during the piston backstroke. The cylinder was machined from Plexiglas, and the piston, skirt, and shaft were made from aluminum. See text for details.

HFV VENTILATOR SERVO CONTROLLER BLOCK DIAGRAM



- R - input waveform
- Offset - DC signal to adjust piston position at end-stroke
- K₁ - forward gain
- G_p - "plant" transfer function, including power amplifier, linear motor, piston/cylinder, and position transducer
- C - position signal
- K_{2s} - idealized velocity feedback
- K₃ - position feedback

Fig. 3. Simple idealized second order feedback system used for ventilator controller. Both position and velocity feedback were required to produce desired performance characteristics. First the actual transfer functions for the "plant" and differentiator blocks were determined, then the values for the gains K₁, K₂, and K₃ were specified by a state variable feedback analysis.

where s is the complex variable $\sigma + j\omega$ used for frequency domain analysis [11].

The servo circuit is diagrammed in Fig. 3. Position, velocity, dc offset, and input signals, with appropriate signs, were summed and the resulting error signal multiplied by a gain factor and output to the power amplifier. The offset control added a dc voltage to the input which moved the piston starting position, allowing the piston to be advanced so that there was no dead space in the chamber at the top of the stroke. The output stage consisted of a 200 W power amplifier built on a printed circuit board designed and kindly provided by J. Lehr of the Harvard School of Public Health, and capable of peak currents of 35 A into a 1 Ω load.

To determine the appropriate gains for optimum performance a state variable feedback analysis was performed. First, the open-loop frequency response of the motor with piston, cylinder, and position transducer attached was measured. This was done by varying the input voltage to the power amplifier to get constant amplitude piston displacement over the frequency range indicated. Gain (output of the position transducer/input voltage) in decibels and phase were measured directly with a Hewlett Packard Gain-Phase Meter (Fig. 4). The phase portion of the transfer function has no significance for this particular application. Examination of this result suggested the "plant" could be modeled as a second-order system:

$$G_p = \frac{K\omega_n^2}{s^2 + 2\zeta\omega_n s + \omega_n^2} \quad (2)$$

The parameters K , ω_n , and ζ were estimated directly from the asymptotic Bode plot, as seen in Fig. 4. The corner frequency of about 10 Hz gave a natural frequency $\omega_n = 2\pi(10)$ rad/s, and the low frequency asymptote of about 11 dB gave a low frequency gain $K = 3.5$. Finally, the damping ratio ζ was estimated from the Bode plot to be approximately 0.8. Putting these values into (2) gave the transfer function for the plant:

$$G_p = \frac{13800}{s^2 + 99s + 4000} \quad (2b)$$

Note that this transfer function includes the power amplifier, linear motor under fully configured (but unloaded) conditions, and the position transducer.

The model used for the state variable feedback analysis is shown in Fig. 5. G_p and G_d are the transfer functions of the motor and piston assembly and the differentiator, as described above. K_1 , K_2 , and K_3 are the gains of the forward, velocity, and position paths, respectively. The closed-loop transfer function for this system is thus

$$\frac{C(s)}{R(s)} = \frac{K_1 G_p}{1 + K_1 K_3 G_p + K_1 K_2 G_p G_d} \quad (3)$$

The goal of this analysis is to determine the values of the constants K_1 , K_2 , and K_3 which will give the desired closed-loop performance. We chose the damping ratio $\zeta = 0.71$ (slightly underdamped as a trade off between quick step response and minimal overshoot), a damped natural frequency $\omega_d = 2\pi(60)$ rad/s (about twice our maximum expected operating frequency), and a dc gain of unity, or

$$\left. \frac{C(s)}{R(s)} \right|_{s=0} = 1$$

the standard form for the ideal second order system is thus

$$\frac{C(s)}{R(s)} = \frac{(2\pi 60)^2}{s^2 + 2(0.71)(2\pi 60)s + (2\pi 60)^2} \quad (4)$$

To solve for the desired constants, insert the expressions for G_D and G_p [(1) and (2b)] into (3) and equate like terms to yield: $K_1 = 10.3$, $K_2 = 0.96$, and $K_3 = 0.97$. Using these gain values yielded

OPEN LOOP FREQUENCY RESPONSE

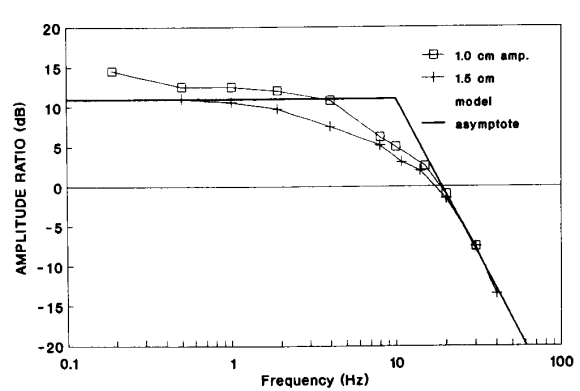
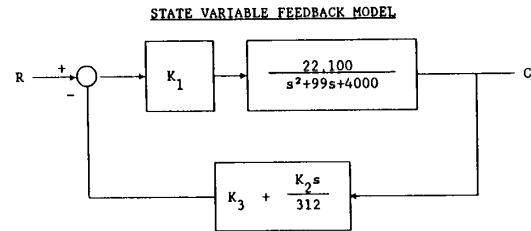


Fig. 4. Open-loop frequency response of the ventilator "plant," consisting of the power amplifier, linear motor, piston/cylinder, and the position transducer. Amplitude ratio (arbitrary units) and phase were measured with the pump unloaded at constant amplitude (1 and 1.5 cm) oscillation. The data were reasonably well modelled as a second order system, as indicated by the superimposed asymptotic and exact Bode plots (solid lines). See text for details.



$$\text{where: } G_p = \frac{22,100}{s^2 + 99s + 4000} \quad G_d = \frac{K_2 s}{312}$$

Fig. 5. State variable feedback model used to determine optimal values for gains K_1 , K_2 , and K_3 . See text for details.

excellent closed-loop performance, as shown in the Bode plots of Fig. 6. Of interest, the gain values obtained by trial and error, while trying to optimize the step response observed on an oscilloscope, were nearly identical to those calculated above.

PERFORMANCE

The ventilator was tested by measuring its tidal volume output under three conditions: no load and loaded with a 6 or a 7 mm i.d. standard endotracheal tube. Delivered tidal volume was measured by directing the ventilator output into a plethysmograph, a large (200 L) rigid box in which pressure oscillations are proportional to the input volume, assuming adiabatic conditions [1], [8]. Since the different loading conditions simulate a changing "respiratory system" impedance, ventilator output was plotted as a function of the changing load impedance according to the model of Venegas [1]:

$$\frac{|Z_l|}{|Z_o|} = \frac{V_{io} \times \Delta P_p}{\Delta P_{po} \times V_l}$$

ΔP_p and ΔP_{po} are the pressure amplitudes measured in the ventilator proximal to the outlet under loaded (ΔP_p) and unloaded (ΔP_{po}) conditions. V_l and V_{io} are the tidal volumes measured in the plethysmograph under loaded (V_l) and unloaded (V_{io}) conditions. $|Z_l|$ and $|Z_o|$ represent the magnitudes of the load impedances, again with endotracheal tube load (Z_l) or unloaded (Z_o). These measure-

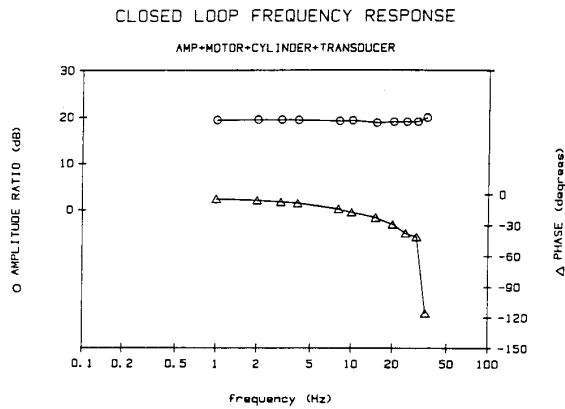


Fig. 6. Closed-loop frequency response for unloaded ventilator at 1.3 cm amplitude stroke, using constants determined by state variable analysis.

ments were performed using sinusoidal oscillations over frequencies ranging from 8 to 27 Hz and tidal volumes of 20 to 50 mL. Pressures were recorded with Validyne DP45 pressure transducers and the signals acquired on a Compaq Portable Computer equipped with a DT2801 A/D converter (Data Translation, Marlboro, MA) and stored for later analysis. The frequencies and peak-to-peak amplitudes of the signals were determined by a curve fitting routine based on the method of least squares [12].

The results are presented in Fig. 7, which plots the delivered V_T , normalized to the "no load" V_{T0} , as a function of the ratio of the normalized impedances $|Z_L|/|Z_0|$ for V_{T0} of 40 mL. Two important phenomena are noted here. First, as frequency increases there is a progressive loss of delivered tidal volume, and this loss increases at higher loads. The maximum loss at $V_{T0} = 40$ mL ranges from less than 10% at 16.5 Hz to 35% at 27.3 Hz. Second, and perhaps more interestingly, there is an "amplification" effect in which the delivered V_T actually surpasses that at no load, and this effect depends on all three factors f , V_{T0} , and Z_L .

DISCUSSION

In this communication we have described the design, construction, and performance of an oscillatory HFV ventilator. The ventilator's mechanical design features the use of frictionless rolling diaphragms in a novel back-to-back configuration which provides a perfect seal while minimizing friction and alignment problems. The leak-proof design is particularly useful to investigators studying HFV with radioactive tracers since there is no loss of activity through the piston. While we used a relatively small diaphragm (45 cm² area), they are available in a wide range of sizes [10] and the same design may be scaled to any size.

A linear motor was used to drive the piston. These types of motors have been used before: in the cardiovascular laboratory to instantaneously change ventricular loading and measure vascular impedances [9], [13], and in similar high frequency ventilators for experimental purposes [3], [14]. Those ventilators, however, were not formally characterized. The ventilator described here uses the same basic arrangement as these other HFV ventilators but features an improved piston design. The linear motor ventilator is quiet, has few moving parts, and has the ability to eliminate all the cylinder dead space and follow any input waveform (with any I:E ratio).

A second order feedback control system was selected for piston position control. We estimated the open-loop transfer function of the real components, proposed a particular solution to the control system problem, and performed a state variable analysis to determine the feedback parameters needed to obtain the desired closed-loop performance. Other high frequency ventilators have used feedback control systems, but they have empirically set their gains

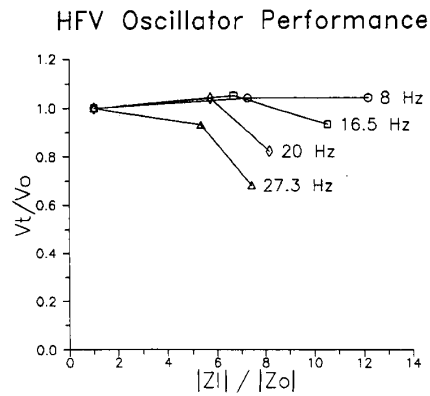


Fig. 7. Performance of high-frequency ventilator using impedance model of Venegas [1]. Normalized tidal volume (V_T/V_{T0}) is plotted against normalized load impedance ($|Z_L|/|Z_0|$) for $V_{T0} = 40$ mL and frequency range 8–27 Hz.

to get "optimum" step response as determined by eye on an oscilloscope (Lehr, personal communication). We have presented a simple quantitative technique to optimize performance of this system which may be easily applied to other control systems in the physiology laboratory.

Ventilator performance was evaluated using the impedance model of Venegas [1], which utilizes simple Thevenin equivalent models of the ventilator and respiratory system load. The analysis showed our ventilator to be of relatively high internal impedance, meaning that ventilator output is relatively independent of loading, with a fall off in performance at higher oscillatory frequencies and loads. This ventilator compares well to the HIFI (high-impedance flow-interrupting) ventilator of Venegas [1] up to 10 Hz, the frequency range tested in that study. No data are available for comparison at higher frequencies. The fall off in delivered V_T at higher frequencies, V_{T0} , and loads is likely due to compression of the gas in the piston and delivery tube proximal to the endotracheal tube. The volume of compressible gas in the ventilator delivery tubing is approximately 100 mL, which with peak pressures ranging from 25 to 150 cm H₂O at a V_{T0} of 40 mL accounts for a maximum of 12 mL of lost tidal volume.

In addition, we noted that the delivered tidal volume can actually increase under certain loading conditions. A similar phenomenon has been described by Brusasco *et al.* [15], who attributed the effect to a combination of gas compression and resonance in the HFV delivery circuit and successfully modelled it using an electrical analog. The absence of this effect in the data of Venegas [1] reflects the fact that there was no piston or compressible dead space volume in their system. Thus, it is important to realize that other factors besides piston displacement may effect delivered tidal volume, and we recommend that an independent measurement of tidal volume, such as a pneumotachograph or plethysmograph, be used when precise control of this variable is desired.

ACKNOWLEDGMENT

The author thanks Dr. W. Mitzner for valuable support and guidance, and E. Shivoder, J. Howell, D. Rabold, and C. Ray for technical assistance. Dr. J. Venegas contributed helpful discussion and criticism. Dr. S. Corrsin provided the linear motor and J. Lehr the power amplifier circuit board.

REFERENCES

- [1] J. G. Venegas, "Equivalent circuit analysis of high-frequency ventilators including a new high-impedance flow-interrupting ventilator," *IEEE Trans. Biomed. Eng.*, vol. BME-33, pp. 420–427, 1986.

- [2] D. J. Bohn, K. Miyasaka, B. E. Marchak, W. K. Thompson, A. B. Froese, and A. C. Bryan, "Ventilation by high-frequency oscillation," *J. Appl. Physiol.: Resp. Environ. Exer. Physiol.*, vol. 48, pp. 710-716, 1980.
- [3] T. H. Rossing, A. S. Slutsky, J. L. Lehr, P. A. Drinker, R. Kamm, and J. M. Drazen, "Tidal volume and frequency dependence of carbon dioxide elimination by high-frequency ventilation," *N. Eng. J. Med.*, vol. 395, pp. 1375-1379, 1981.
- [4] G. G. Weinman, W. Mitzner, and S. Permutt, "Physiological dead space during high-frequency ventilation in dogs," *J. Appl. Physiol.*, vol. 57, pp. 881-887, 1984.
- [5] P. R. Fletcher, M. A. Epstein, and R. A. Epstein, "A new ventilator for physiologic studies during high frequency ventilation," *Resp. Physiol.*, vol. 47, pp. 21-37, 1982.
- [6] D. Goldstein, A. S. Slutsky, R. H. Ingram Jr., P. Westerman, J. Venegas, and J. Drazen, "CO₂ elimination by high frequency ventilation (4 to 10 Hz) in normal subjects," *Amer. Rev. Resp. Dis.*, vol. 123, pp. 251-255, 1981.
- [7] Y. K. Ngeow and W. Mitzner, "A new system for ventilating with high-frequency oscillation," *J. Appl. Physiol.: Resp. Environ. Exer. Physiol.*, vol. 53, pp. 1638-1642, 1982.
- [8] B. A. Simon, G. G. Weinmann, and W. Mitzner, "Mean airway pressure and alveolar pressure during high-frequency ventilation," *J. Appl. Physiol.: Resp. Environ. Exer. Physiol.*, vol. 57, pp. 1069-1078, 1984.
- [9] H. Suga and K. Sagawa, "End-diastolic and end-systolic ventricular volume clasper for the isolated canine heart," *Amer. J. Physiol.*, vol. 233, pp. H718-H722, 1977.
- [10] *Bellofram Diaphragm Design Manual*. Burlington, MA: Bellofram Corp., 1980.
- [11] B. C. Kuo, *Automatic Control Systems*. Englewood Cliffs, NJ: Prentice-Hall, 1982.
- [12] B. A. Simon, "The dynamic distribution of pulmonary ventilation during high frequency ventilation," Ph.D. thesis, Johns Hopkins Univ., Baltimore, MD, 1987.
- [13] D. K. Bogen, Y. Ariel, T. A. McMahon, and W. H. Gaasch, "Measurement of peak systolic elastance in intact canine circulation with servo pump," *Amer. J. Physiol.*, vol. 249, pp. H585-H593, 1985.
- [14] A. S. Slutsky, R. D. Kamm, T. H. Rossing, S. H. Loring, J. Lehr, A. H. Shapiro, R. H. Ingram Jr., and J. M. Drazen, "Effects of frequency, tidal volume, and lung volume on CO₂ elimination in dogs by high frequency (2-30 Hz) low tidal volume ventilation," *J. Clin. Invest.*, vol. 68, pp. 1475-1484, 1981.
- [15] V. Brusasco, K. C. Beck, M. Crawford, and K. Rehder, "Resonant amplification of delivered volume during high-frequency ventilation," *J. Appl. Physiol.*, vol. 60, pp. 885-892, 1986.

Piezoelectric Effect in Renal Calculi

V. R. Singh, Ravinder Agarwal, and Ved Singh

Abstract—The piezoelectric effect is investigated for the first time in renal calculi *in vitro*. The kidney stones are shaped from solid samples as well as from stones crushed into powder and pressed into tablets. Presence of alpha quartz in the renal calculi is investigated by an X-ray technique and the presence of this constituent also helps to explain the piezoelectric effect in the renal calculi. The dielectric and piezoelectric parameters are studied in detail.

INTRODUCTION

Various mechanical, chemical, ultrasonic, and electrical characteristics of renal calculi, viz. kidney stones, have been studied

Manuscript received October 13, 1989; revised May 29, 1990.
The authors are with the National Physical Laboratory, New Delhi 110 012, India.
IEEE Log Number 9041291.

to determine the design parameters for an ultrasonic lithotripter [1]-[3]. In the present work, measurements have been made of the electrical (resistivity), dielectric (dielectric constant, dissipation factor), and piezoelectric (charge constant and voltage constant) properties of the experimental samples made from solid kidney stones as well as from powdered stones. The kidney stones are found to exhibit the property of piezoelectricity.

Kidney stones are also studied for their chemical composition to find the presence of various constituents like calcium oxalate, calcium phosphate, calcium carbonate, magnesium potassium phosphate, and uric acid. The presence of α -quartz has been observed from X-ray analysis first time in this work.

MATERIAL AND METHOD

A. Dielectric Study on Natural Kidney Stones

The kidney stones were obtained from local hospitals. After biopsy, stone specimens were allowed to dry for a month and then machined. Electrical contacts were provided by using air-dry silver paste on either side of the kidney stone for electrical measurements. After proper silvering, the specimens were poled at dc electric field of 10 to 12 kV/cm at an elevated temperature of 150°C. The measurements of piezoelectric properties were made for both poled and unpoled samples.

B. Dielectric Study on Powdered Kidney Stones Tablets

The specimens collected from different hospitals were crushed into powdered form. The powder thus obtained was ground by dry ball-milling for 12 h. The stone powder was mixed with a few drops, viz. 2-3%, of polyvinyl alcohol (PVA) and compressed into the circular tablets having a diameter of 19 mm and a thickness of 3 mm. These tablets were allowed to dry for ten days and then an electroded with air-dry silver paste on either side and poled by applying dc electric field of 8 to 9 kV/cm at elevated temperature of 80-90°C (to keep the PVA from dissolving and not causing a permanent changes in its characteristics). Measurements were then made both on poled and unpoled samples.

C. X-Ray Diffraction Study

The stones were crushed to fine powder in an agate pestle and mortar. The fine powder was filled in the circular cavity of the specimen holder and was compressed with a glass slide using thumb pressure. The specimen holder was then inserted into a support for the specimen holder of the diffractometer. A Siemens D-500 diffractometer was used to investigate the crystalline phases.

D. Measurements

The measurements of electrical and piezoelectric parameters at room temperature were made two days after the samples were poled to decrease the effects of aging. The measurement of capacitance and dielectric loss factor ($\tan \delta$) at 1 kHz was made by using a precision impedance (LCR) bridge. The resistivity was measured using an ohm-meter (million megohmmeter) model RM 160 MK III BPL, India). The piezoelectric charge constant (d_{33}) was measured by using an Aerotech "d₃₃" Tester (model A-2). The dielectric constant was then determined by using the relationship

$$K_{33}^T = \frac{C \cdot t}{0 \cdot 0885 \cdot A}$$

where t is thickness (cm) of the sample, A is the area (cm²), and C the capacitance (pF). Voltage constant g_{33} was calculated from the measured value of charge constant and dielectric constant by